



Investigation of the Effect Mechanism of Cutting Sequence on Spiral Milling of CFRP/Ti Laminates Under Ultrasonic-Assisted Conditions

Kai Yang^{1,2} · Jie Pan³ · Ziyang Cao^{1,2} · Yiwen Zhu^{1,2}

Received: 22 August 2023 / Revised: 7 January 2024 / Accepted: 8 January 2024 / Published online: 1 February 2024
© The Author(s), under exclusive licence to Korean Society for Precision Engineering 2024

Abstract

The hole-making mechanism of carbon fiber reinforced plastic (CFRP)/titanium alloy stacks is different from that of monolayer materials. In order to reveal the effects of different cutting sequence strategies on the hole-making quality and machining efficiency of the stacked materials, valuable insights are provided for the design of the stacking machining process and the selection of the most suitable cutting sequence. The researchers conducted ultrasonic vibration-assisted helical milling and conventional helical milling experiments with different milling parameters, and explored the basic influence mechanisms of CFRP → Ti and Ti → CFRP on the hole-making in both ways. The results show that different cutting sequences have significant effects on the axial force and chip morphology changes during CFRP/Ti stack machining. The dimensional accuracy and consistency of the holes cut from the Ti side are better, and the quality of the entrance and exit from the Ti side under the ultrasonically assisted condition is close to the quality level of the holes cut from the CFRP side under the normal helical milling, and the ultrasonically assisted condition plays a good role in improving the quality of the holes made. In addition, the tearing coefficients of CFRP hole entry/exit in both machining modes increased with the increase of feed per tooth in tangential direction and decreased with the increase of spindle speed. The tearing coefficients of entry/exit holes in CFRP direction were smaller than those in titanium direction.

Keywords CFRP/Ti stacks · Spiral milling · Cutting sequence · Ultrasonic vibration-assist · Hole-making quality

Kai Yang and Jie Pan have contributed equally to this work.

✉ Ziyang Cao
dukeczy@nuaa.edu.cn

Kai Yang
m17851145107@163.com

Jie Pan
p13685298420j@163.com

Yiwen Zhu
15358446337@163.com

- ¹ College of Mechanical Engineering, Suzhou University of Science and Technology, Suzhou 215009, China
- ² Suzhou Key Laboratory of Precision and Efficient Machining Technology, Suzhou 215009, China
- ³ Changzhou Branch of Jiangsu Union Technical Institute, Changzhou 213032, China

1 Introduction

With the rapid development of aerospace technology, titanium alloys and carbon fiber reinforced composites (CFRP) are widely used to manufacture aerospace products for their excellent comprehensive performance [1–3]. CFRP has the characteristics of low density, high specific modulus, high specific strength, strong designability, and ease of integrally molded in a large area [4–8]. Titanium alloys have high strength, good thermal stability, and corrosion resistance [9, 10], and both are often used in the form of lamination in the aircraft manufacturing process.

The laminated material composed of CFRP and titanium alloy has good complementarity and chemical compatibility, is lightweight and high strength, and meets the requirements of strength and stiffness performance while having excellent structural quality and environmental performance, effectively avoiding the problems of low impact strength and irreparable problems of composite materials [11, 12]. In the new generation of aerospace manufacturing, CFRP/Ti stacks, the preferred material for high-performance structural

components, have gradually replaced the traditional CFRP and titanium alloy single application [13, 14]. During manufacturing and assembly, the laminated structures are usually connected in three forms: mechanical connection, glued connection, and hybrid mechanical/glued connection [15, 16]. Mechanical linkages are robust, reliable, and easy to disassemble. CFRP and titanium alloys are often mechanically connected to form their structures, and the quality of connection holes determines the stacked materials' performance. To guarantee the assembly accuracy of the stacked holes, both materials are usually machined simultaneously using one tool [17–19]. Titanium alloy and CFRP are challenging materials to machine, each with distinct machining characteristics. When hole-making in stacked layers, they are susceptible to significant machining damage, which leads to part scraps, such as interlayer delamination, fiber tearing, entrance and exit burrs, and other defects [20–22]. To obtain the required hole diameter and machining quality, researchers, both domestically and internationally, have undertaken numerous investigations on hole-making technology for CFRP/Ti stacks, exploring various aspects like machining techniques, cutting parameters, tool materials, and cutting environments [23–26].

Most studies on CFRP/titanium alloy laminated materials' hole-making technology center primarily around conventional drilling. However, based on the fact that the traditional drilling hole-making process has the problems of chips not easy to be discharged, tool wearing too fast, and tool tip temperature too high, the research scope of drilling laminated materials is getting narrower and narrower, which can not fully satisfy people's requirements of high efficiency, high machining accuracy and low damage for CFRP/titanium alloy laminated materials hole making. Simultaneously, researchers in academia and industry have shown significant interest in developing helical milling hole-making. Spiral milling is a new type of hole-making method that adopts the principle of milling to realize hole machining; the tool rotates around the hole axis at the same time as the rotation. It makes eccentric movement around the trajectory of the helix under the action of axial feed, and the cutting process includes the intermittent cutting of the peripheral edge and the continuous cutting of the end edge, with the intermittent cutting of the peripheral edge dominating [27, 28]. Domestic and foreign scholars, through a large number of drilling and milling comparative studies, found that: the spiral milling intermittent cutting process is conducive to tool heat dissipation, eccentric movement of the machining mode is conducive to the timely discharge of chips, and compared with the traditional drilling has the advantages of small axial force, good machining quality, and low cost of cutting tools, which is of practical effect and application value for the study of hole making problems in CFRP/Ti stacks [29, 30]. In addition, ultrasound-assisted machining technology

can significantly improve the machinability of materials and is often used in the field of hard and brittle materials and other difficult-to-machine materials [31–33]. Some scholars have attempted to apply ultrasound-assisted machining technology to make holes in CFRP/Ti stacked materials. Cong et al. [34, 35] conducted a preliminary investigation of rotary ultrasonic machining (RUM, Rotary Ultrasonic Machining) of CFRP/Ti stacks. They compared the rotary ultrasonic machining of drilled holes with the literature results of using other methods. They discovered that the cutting force exhibited a decrease, resulting in improved hole quality. Yan Chen et al. [36] conducted a low-frequency vibration-assisted drilling (LFVAD) study on CFRP/Ti stacks, which demonstrated that the adaptive LFVAD process is significantly more effective than the traditional LFVAD process in improving tool wear and machining efficiency. Onawumi et al. [37] found in experiments on ultrasonically assisted drilling (UAD, Ultrasonically Assisted Drilling) of CFRP/Ti laminated materials that the reduction of axial force by UAD decreases with the increase of the feed rate, but the improvement of UAD on the roundness error of the holes and the height of the burr is still significant. The reduction of the burr is about 50% compared with regular drilling. The findings above suggest that ultrasonic-assisted machining technology holds promising potential for reducing cutting forces and enhancing hole-making quality. Until now, the predominant focus of research on ultrasonic machining of holes in CFRP/Ti stacks has been primarily on drilling holes. There are limited reports on the utilization of helical milling technology in the existing literature. Consequently, whether ultrasonically-assisted machining can enhance the machinability of spiral milling holes in CFRP/Ti stacks remains to be seen.

The hole-making process of CFRP/Ti stacks involves two cutting sequences, and the selection of the cutting sequence greatly influences the laminated holes' dimensional accuracy and overall machining quality. Because of CFRP's weak interlayer bonding strength, the titanium alloy can act as a supportive mat during the CFRP → Ti cutting sequence. This sequence exhibits a higher critical axial force compared to the Ti → CFRP cutting sequence, which, in turn, reduces exit delamination and tearing damage to a lower extent. However, the CFRP → Ti cutting sequence has the problems of scraping the CFRP hole wall when the lower layer of titanium alloy chips is discharged, and tool chip entanglement leads to more significant hole diameter errors in CFRP and increased tool wear [38]. Conversely, employing the Ti → CFRP cutting sequence enhances the efficient removal of titanium alloy chips and facilitates rapid heat dissipation. As a result, this sequence leads to improved hole wall quality and dimensional accuracy, but there is a higher risk of CFRP exit damage when the cutting force is too large. So far, based on the fact

that CFRP delamination and tearing damage are the most important reasons leading to product scrap, the research on CFRP/Ti stacked hole-making is mainly carried out under the sequence of CFRP → Ti, and the feasibility of experimental studies under different cutting sequences has not been widely discussed.

Based on these motivations, this research explores the processing of CFRP/Ti stacks through various cutting sequences, mainly focusing on the cutting axial force, chip morphology changes, and hole-making quality aspects. The study involves ultrasound-assisted spiral milling to assess factors like interface zone damage, CFRP entrance and exit qualities, hole diameter, and roundness. In addition, experiments were carried out in different milling parameter ranges to investigate the trend of hole-making quality as a function of parameters. The research aims to visualize and comprehend the machining response of diverse cutting sequences on holes made in composite/metal stacks. The main objective is to uncover the mechanism behind the impact of different cutting sequences during ultrasound-assisted spiral milling of CFRP/Ti stacks, which in turn can guide the design of the machining process of stacked materials in aerospace and automotive manufacturing industries in order to achieve high-precision hole fabrication and to ensure the quality and performance of components.

2 Theoretical Model

2.1 Forms of Realisation of Ultrasound-Assisted Spiral Milling

2.1.1 Spiral Milling Principle of Operation

Spiral milling is the principle of milling to achieve the new hole-making method of hole machining, the tool in the rotation of the hole axis at the same time around the rotary axis, and in the axial feed under the action of the helical trajectory to do eccentric movement, the cutting process includes the peripheral edge of the intermittent cutting as well as the end of the cutting edge of the continuous cutting to the peripheral edge of the intermittent cutting is dominated by the [26, 27]. As shown in Fig. 1, O_1 is the rotary center of the machining hole work surface, O_2 is the rotary center of the spindle where the tool is located, a is the pitch (the displacement generated by the tool center doing axial feed movement for one week according to the helical trajectory), and θ is the helix angle of the helical trajectory.

In order to elucidate the basic working principle of helical milling, it is first necessary to determine several important

basic parameters in the process of helical milling: spindle speed (rotation speed) n_{rot} (rpm), cutting feed per tooth f_z (mm/z), pitch e (mm). Assuming that the tool diameter is D_{tool} (mm), the diameter of the machined hole is D_{hole} (mm), and the number of milling cutter edges is z . Based on the above basic parameters, further definitions can be made for the other parameters in the spiral hole milling process:

The distance between the axial direction of the tool and the axial direction of the machined hole, the eccentricity distance can be expressed as:

$$e = \frac{D_{hole} - D_{tool}}{2} \quad (2.1)$$

The rotational velocity of the tool center around the hole axis can be expressed as:

$$n_{rev} = \frac{f_z \cdot n_{rot} \cdot z}{\pi \cdot (D_{hole} - D_{tool})} \quad (2.2)$$

Since the axial feed speed f_a (mm/min) of the tool satisfies the relationship $f_a = a \cdot n_{rev}$ with the pitch e (mm) and the tool rotational speed n_{rev} (rpm), the axial feed speed of the tool can be expressed by Eq. (2.2) as:

$$f_a = a \cdot n_{rev} = \frac{a \cdot f_z \cdot n_{rot} \cdot z}{\pi \cdot (D_{hole} - D_{tool})} \quad (2.3)$$

Accordingly, the tangential feed rate of the tool can be expressed as:

$$f_t = n_{rot} \cdot f_z \cdot z \quad (2.4)$$

According to Fig. 1, the helix angle of the tool helical trajectory can be expressed as:

$$\theta = \arctan \frac{a}{\pi \cdot (D_{hole} - D_{tool})} = \arctan \frac{f_a}{f_t} \quad (2.5)$$

2.1.2 Side Edge Trajectory

In order to analyse the form of interaction between the tool and the material in the process of spiral milling, and to investigate the motion of the tool in the cutting process, it is necessary to establish the equation of the motion trajectory of the milling cutter at a point on the side edge in the process of spiral milling. Therefore, the $x_1O_1y_1, x_2O_2y_2$ plane rectangular coordinate system is established with the centre of the hole O_1 and the centre of the tool O_2 as the origin, as shown in Fig. 2.

With the axial feed direction of the tool defined as the positive direction of the z-axis, the kinematic analysis of Fig. 2 yields a coordinate expression for the motion trajectory of a point on the side edge of the tool during spiral hole milling:

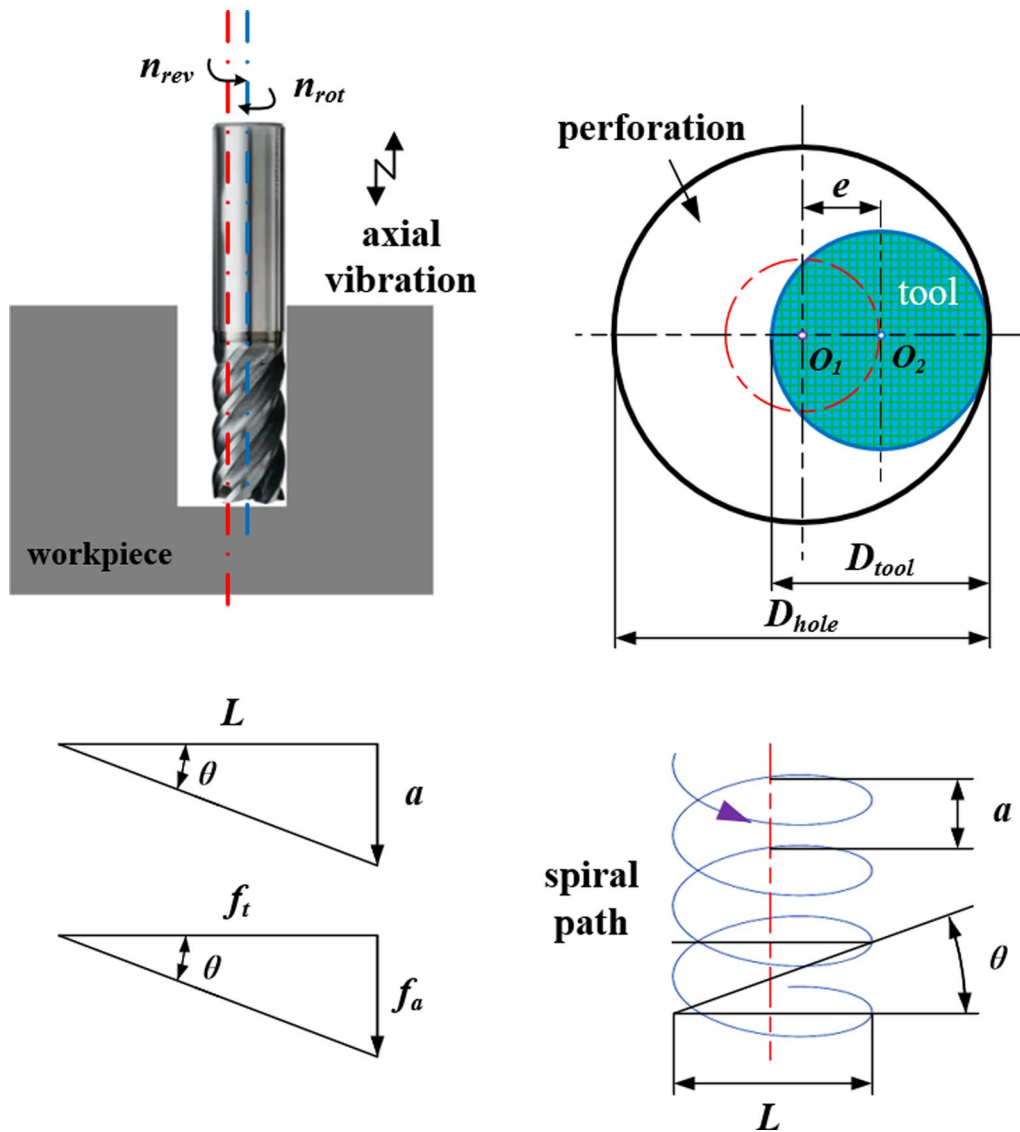


Fig. 1 Schematic diagram of the working principle of spiral milling holes (n_{rot} is rotation speed, n_{rev} is revolution speed)

$$x_{cm} = e \cdot \cos(\omega_{rev}t) + \frac{D_{tool}}{2} \cdot \cos(\omega_{rot}t) \tag{2.7}$$

$$\omega_{rot} = \frac{2\pi \cdot n_{rot}}{60} \tag{2.10}$$

$$y_{cm} = e \cdot \sin(\omega_{rev}t) + \frac{D_{tool}}{2} \cdot \sin(\omega_{rot}t) \tag{2.8}$$

$$\omega_{rev} = \frac{2\pi \cdot n_{rev}}{60} \tag{2.11}$$

$$z_{cm} = z_0 - f_a t \tag{2.9}$$

where z_0 is the initial position of a point on the side edge of the milling cutter before the movement, ω_{rot} is the rotational angular velocity of the cutter, ω_{rev} is the revolution angular velocity of the cutter, and the expressions of ω_{rot} and ω_{rev} are as follows:

The ultrasonic vibration in this paper is generated by applying axial vibration to the tool. Assuming that the ultrasonic frequency is f (Hz) and the ultrasonic amplitude is A (μm), the coordinates of a point on the side edge of the axially ultrasonically assisted helical milled hole in the Z-axis direction are:

$$z_{vm} = z_{cm} + A \cdot \sin(2\pi ft) \tag{2.12}$$

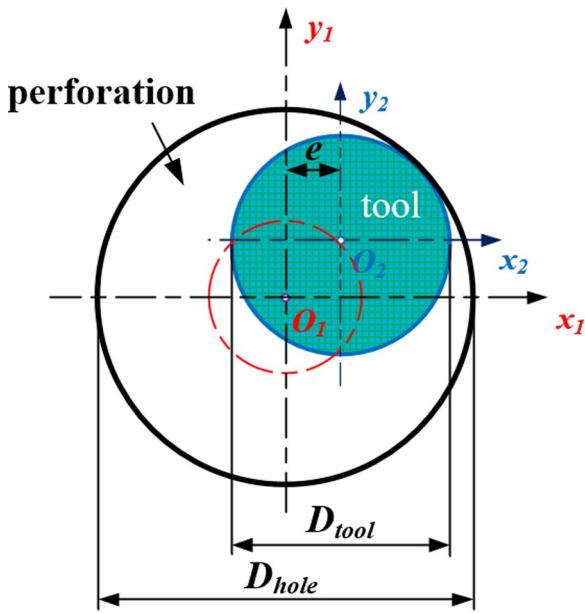


Fig. 2 Spiral milling hole 2D plane diagram

At the same time, the coordinate expression for the motion trajectory of a point on the side edge of the spiral milling tool under ultrasound-assisted conditions can be obtained:

$$x_{vm} = e \cdot \cos(\omega_{rev}t) + \frac{D_{tool}}{2} \cdot \cos(\omega_{rot}t) \tag{2.13}$$

$$y_{vm} = e \cdot \sin(\omega_{rev}t) + \frac{D_{tool}}{2} \cdot \sin(\omega_{rot}t) \tag{2.14}$$

$$z_{vm} = z_{cm} + A \cdot \sin(2\pi ft) = z_0 - f_a t + A \cdot \sin(2\pi ft) \tag{2.15}$$

In order to visually compare the trajectories of the side edges of the helical milling holes with and without ultrasonic assistance, assuming that the cutting conditions are spindle speed $n_{rot} = 5000$ rpm, cutting feed per tooth $f_z = 0.03$ mm/z, and pitch $e = 0.1$ mm, the tool trajectories under the two cutting conditions are plotted, as shown in Fig. 3.

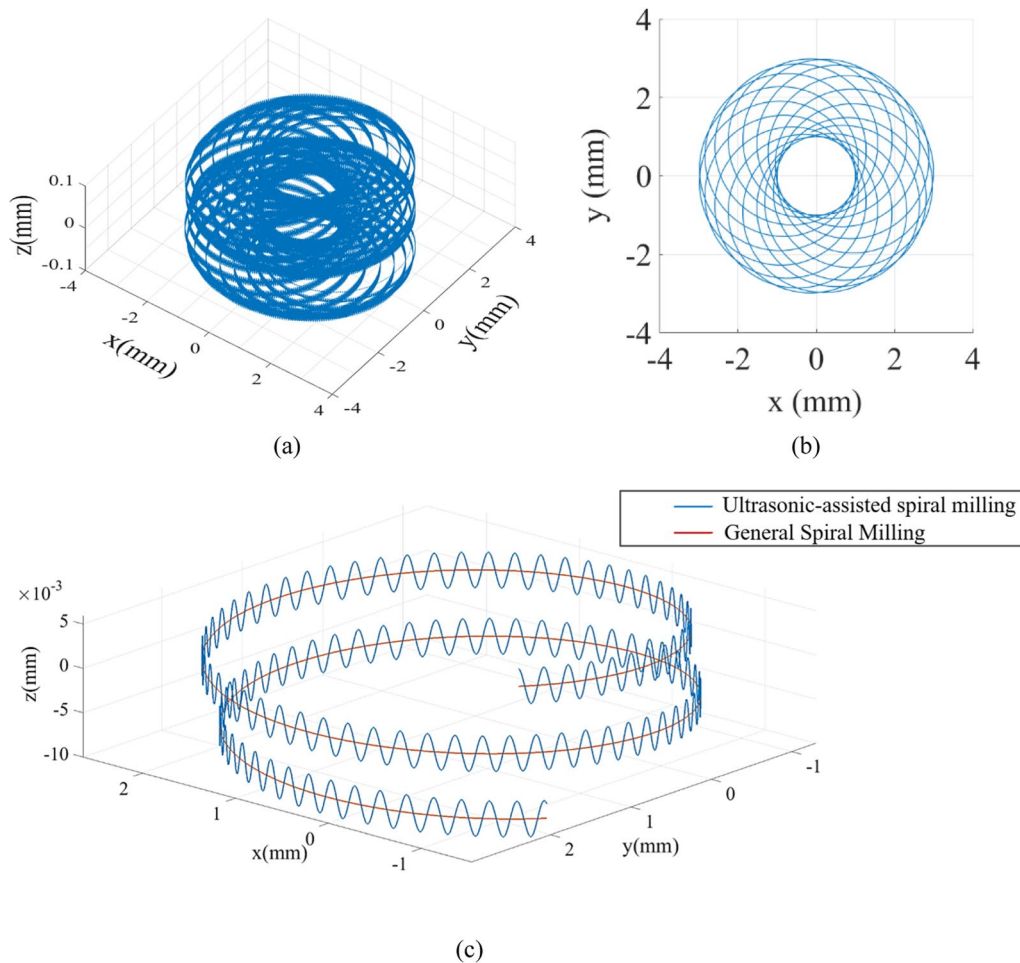


Fig. 3 Motion trajectory diagram of a point of the side edge of the spiral milling tool: a 3D macro trajectory; b 2D macro trajectory; c 3D local trajectory comparison

As can be seen from the figure, the trajectory of a point on the side edge of the milling cutter in the axial direction under ultrasound-assisted conditions is characterized by the periodic motion of a sinusoidal curve. This periodic trajectory is generated by the axial high-frequency vibration of the tool, which enables the tool side edge to produce a superposition effect in the process of cutting, increasing the number of cutting times of the tool on the hole wall, and improving the machining quality of the surface of the hole wall to a certain extent.

2.2 Mechanism of Cutting Sequence Influence on Stacked Hole-Making

From the analysis of the kinematic trajectory of spiral milling holes, it can be seen that the time-varying characteristics of the effective front angle of the side edges under ultrasound-assisted conditions can to a certain extent improve the conditions of chip breakage and chip removal in the process of CFRP/Ti-6Al-4V laminated holes, however, the problem of chip removal of the spiral milling holes still exists, and some of the residual chips inside the holes are still involved in the subsequent removal of the material, which will inevitably have a certain effect on the hole-making quality and tool life during the cutting process.

There are two cutting sequences in the hole making process of CFRP/Ti-6Al-4V laminated materials. The choice of cutting sequence has a significant effect on the dimensional

accuracy and machining quality of the laminated holes. In this section, the chip removal mechanism of titanium alloy under two different cutting sequences is analyzed based on the geometrical model of unaltered chips in the spiral hole milling process. As shown in Fig. 4, with the cutting sequence of CFRP → Ti, the residual chips in the hole contain powdered CFRP chips as well as titanium alloy chips. Among them, the CFRP chips at the bottom of the hole are mainly generated by part of the CFRP chips accumulated near the hole in the previous period, while the titanium alloy chips at the bottom of the hole are mainly formed due to the centrifugal force generated by the high-speed rotation of the tool, which makes part of the chips break away from the chip removal groove and fall into the hole after scraping the CFRP hole wall. Compared with this, the cutting sequence of Ti → CFRP, the centrifugal effect on the spiral groove chip is lower, the chip removal process is more smooth, the residual chips in the hole are only titanium alloy chips, and the residual amount of chips is relatively lower.

From the point of view of unchanged chips, under the Ti → CFRP cutting sequence, relatively less chip residue in the hole means that the tool in the cutting process for the bottom of the residual chip secondary cutting amount is lower, to a certain extent, it represents a relatively lower cutting thickness, that is, the thickness of the unchanged chip is reduced, and thus the cutting force is also smaller. In addition, less chip residue means less chip attachment to the tool surface, and lower friction between the chip and the

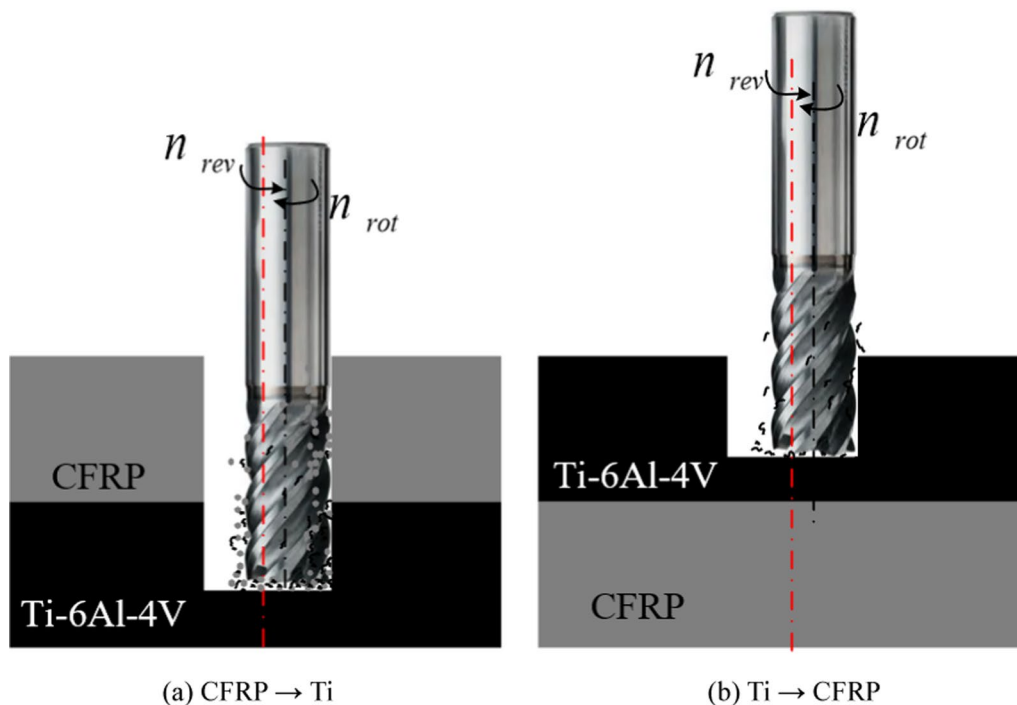


Fig. 4 Chip removal mechanism for different cutting sequences (n_{rot} is rotation speed, n_{rev} is revolution speed)

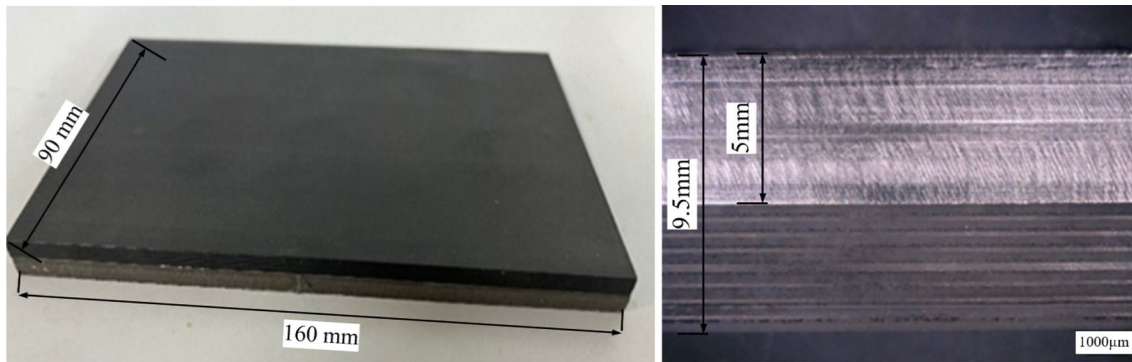


Fig. 5 CFRP/Ti stacks

Table 1 Performance parameters of CFRP and titanium alloys

Material	Tensile strength (MPa)	Elongation (%)	Density (g/cm ³)	Coef- ficient of restitution (GMa)	Poisson's ratio
T700	4900	2.1	1.6	230	0.3
TC4	950	8	4.4	113	0.34



Fig. 6 Experimental tool

front and back of the tool, which helps to reduce tool wear and improve tool life.

3 Experimental Step

3.1 Workpieces and Tools

The stacked workpiece used for ultrasound-assisted spiral hole milling experiments consisted of a T700 epoxy matrix carbon fiber composite and a Ti6Al4V plate. The dimensions were 160 mm × 90 mm, and the thicknesses of the T700 carbon fiber composite and Ti6Al4V plate were 4.5 mm and 5 mm, respectively, as shown in Fig. 5. To achieve a quasi-isotropic structure, the T700 carbon fiber composite was layered multi-directionally in a repeating pattern of [(0°/-45°/45°/90°)]. The room temperature physico-mechanical properties of this composite are detailed in Table 1. The tool used in the experiment is a special end

mill for helical hole milling, as shown in Fig. 6. The tool is a diamond-coated monolithic tungsten carbide end mill with a diameter of 4 mm, a length of 60 mm, four flutes, a helix angle of 35°, a flute length of 12 mm, and a flexural strength of 4500 N/mm². A Ti Al N-coated tool, which is suitable for cutting CFRP and titanium alloys, was selected for this experiment. The cutting edge of this tool has good wear resistance, good toughness and resistance to thermal deformation. During the milling process, the bottom and side edges of the tool are involved in cutting at the same time, the bottom edge is mainly involved in axial feed, and the side edges are mainly involved in the processing of the hole wall.

We should also note that when using the ultrasonic vibratory milling method of hole making, the depth of cut is not constant but varies periodically. Studies have shown that the average axial force is significantly reduced when using this hole-making method compared to the typical drilling method. Due to the unique cutting mechanism of ultrasonic vibration milling holes, the cutting axial force signal will also show a cyclic change with the periodic displacement of the tool. The drilling force signal of ordinary drilling will also fluctuate within a specific range. Hence, this paper carries out an average filtering process on the collected axial force signal to prevent pulse interference from obtaining the average axial force, which also eliminates the influence of occasional pulse interference on the measurement to a specific degree value.

3.2 Experimental Conditions and Program

3.2.1 Experimental Condition

The whole milling hole-making experimental system is shown in Fig. 7; the working platform used for the experiment is JDVT600 A13s Beijing fine engraving machine, with ultrasonic tool holder to realize ultrasonic-assisted milling. The ultrasonic longitudinal vibration system consists of

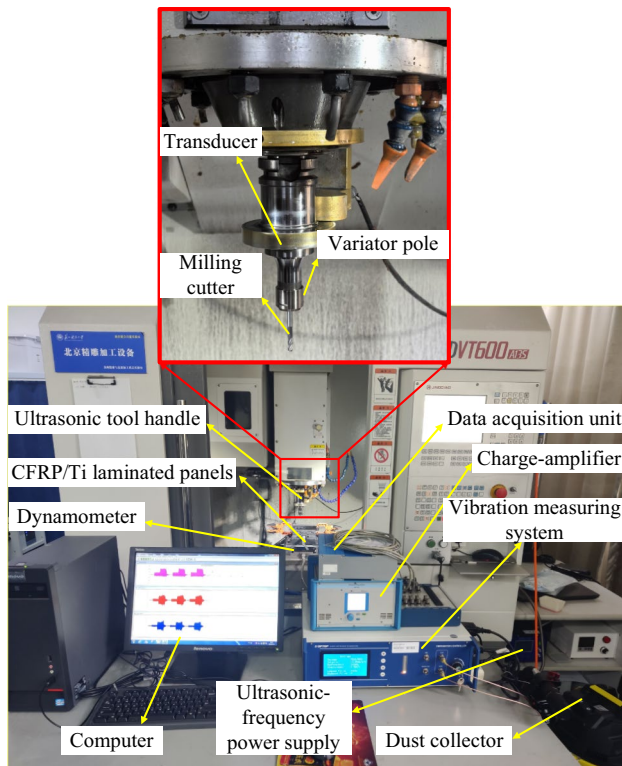


Fig. 7 Experimental system for milling and hole making

a vibration source (ultrasonic generator), a transducer and an amplifier rod. Its vibration frequency is 21.88 kHz, vibration mode for axial vibration milling. The measurement of axial forces during milling is realised by fixing the workpiece to the Kistler 9257B force gauge using a fixture, via a data acquisition card to a charge amplifier and finally to a computer terminal. The experimental process used dry cutting and turning on an industrial vacuum cleaner to absorb the carbon fiber powder debris generated by the milling process. After completing each set of experiments, the milling process yielded titanium alloy chips. We collected and sorted these to enable a detailed analysis of how the cutting sequence affected the chip morphology.

3.2.2 Experimental Program

This paper focuses on the effect of cutting sequence (i.e., CFRP → Ti and Ti → CFRP) on the characteristics and damage mechanisms of ultrasonically-assisted spiral milling of holes in CFRP/Ti laminated materials under different cutting parameter conditions and whether ultrasonic machining contributes positively to the quality of the holes machined. To reduce the influence of tool wear on the experimental outcomes, we limited each tool's usage to only three sets of experiments. We repeated each set of cutting parameters

Table 2 Cutting sequence experimental machining conditions and parameter levels

Parameters	Level
Spindle speed n (r/min)	4000/5000/6000/7000
Tangential feed per tooth f_z (mm/z)	0.01/0.03/0.05/0.07
The pitch of spiral a (mm)	0.1
Eccentricity e (mm)	1
Vibration frequency f (KHz)	21.86
Amplitude A (μm)	10
Cutting sequence	CFRP → Ti, CFRP → Ti
Cooling method	Dry cutting

three times to calculate average values for further analysis. Following the milling experiments, we employed a Coordinate measuring machine (CMM) to inspect hole characteristics, including diameter and roundness errors. Furthermore, a VHX-2000C ultra-large depth-of-field microscope was used to observe the quality of the hole entrance and exit and the hole wall. Based on the available experimental conditions and the representative range of stack milling parameters in the relevant literature, as well as the selected tool parameters, Table 2 lists the machining parameters for the hole milling tests.

4 Results and Analysis

4.1 Effect of Cutting Sequence on the Axial Force of Cutting

Examining axial force is essential in investigating hole-making processes in CFRP/Ti laminates. To compare the axial force differences between the two machining methods during hole-making, we used experimental data to plot the variation curves of axial force overtime for spiral milling of holes under both unassisted and ultrasonically-assisted conditions, with $n = 5000$ r/min and $f_z = 0.03$ mm/z. The corresponding results are illustrated in Fig. 8.

As shown in Fig. 8a, the axial force exhibits five distinct stages throughout the entire cutting process when cutting from the CFRP side. In stage A–B, the bottom edge of the tool gradually cuts into the CFRP layer, which is manifested by the beginning of a gradual increase in the cutting force. In stages B–C, the bottom edge of the tool cuts into the CFRP interior and enters a stable cutting state, shown in the figure, as the cutting force remains constant and steady. In stages C–D, as the tool moves through the CFRP layer and reaches the transition region before entering the Ti–6Al–4V layer, a sudden change in cutting force occurs due to the distinct material properties. At this point, the bottom edge of the tool has not fully penetrated the titanium alloy, leading to a

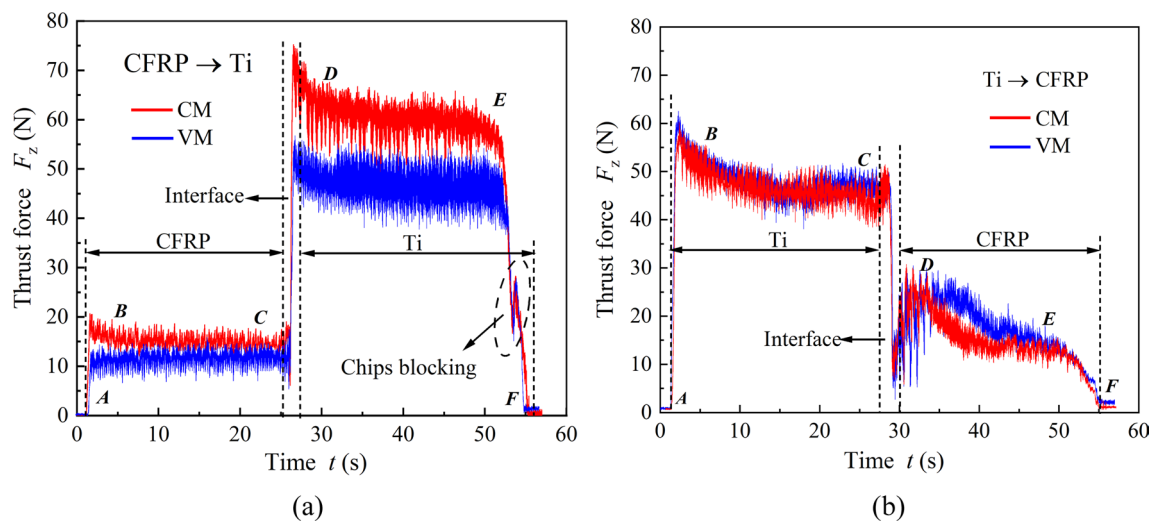


Fig. 8 Comparison of axial force in a single hole for different cutting sequences: **a** CFRP → Ti and **b** Ti → CFRP

rapid force variation. When cutting through the composite material, the rebound effect of the titanium alloy exerts an impact on the tool, resulting in relatively high axial forces during the initial entry into the titanium alloy. In stages D–E, the cutting process stabilizes as the cutting depth increases, reaching the point where the tool thoroughly penetrates the titanium alloy layer. Consequently, the cutting force decreases and remains constant at a stable level. In stage E–F, as the tool approaches the end of the milling process through the titanium alloy layer, the cutting force reduces due to the workpiece's weakened strength. It is worth noting that there is a period of cutting force abnormality in this stage, due to the titanium alloy without adding a pad underneath the tool is about to cut out the titanium alloy layer, the decline in the strength of the workpiece coupled with serious tool wear, cutting edge blunt, cutting ability to reduce the cutting force increases, cutting temperature rises, resulting in the workpiece material plastic deformation of the region increases, the workpiece bottom surface material gives way, resulting in fluctuations in the cutting force.

By comparing the normal and ultrasonic axial forces in the CFRP → Ti direction, we observe a substantial reduction in the average axial force during the ultrasonic-assisted spiral hole milling process for both CFRP and titanium alloy cutting phases. The CFRP experiences a 26.2% reduction in average axial force, while the titanium alloy shows a 22.8% decrease. This is because the ultrasonic vibration turns the continuous cutting process into high-frequency separated cutting, and the effective front angle of the circumferential cutting edge has time-varying characteristics to reduce the friction between the shear force in the first deformation zone and the chips, which promotes the chip breaking and chip removal and reduces the phenomenon of sticking tools. In addition, the fluctuation of axial force under

ultrasound-assisted conditions is more extensive, which is more significant in the cutting stage of titanium alloy. This phenomenon can be attributed to the frequent contact and separation between the tool and the workpiece during ultrasonic-assisted cutting, combined with the continuous variation in cutting thickness [39]. Notably, the axial force in the interface zone of the regular spiral milling hole exhibits a significant local peak due to the substantial material property difference between CFRP and titanium. However, the axial force transition in the interface zone of the stacked material under ultrasonic-assisted conditions is more consistent. It lacks localized sudden increases observed in the regular spiral milling hole. This difference in axial force behavior highlights the distinct effects of ultrasonic assistance on the milling process.

As shown in Fig. 8b, when cutting from the Ti6Al4V layer, the cutting process is stable, and the chip removal is smooth. On the contrary, when cutting from the CFRP layer, the stability and chip removal efficiency gradually decreases. This phenomenon is attributed to the direct separation of Ti6Al4V chips from the hole without contacting or scratching the CFRP layer. Additionally, the powdered chips produced during CFRP cutting do not impact the machined surface of the Ti6Al4V layer when holes are cut through the underlying CFRP material [18].

When comparing regular and ultrasonic axial forces in the direction from Ti to CFRP, the study found that both machining modes exhibited similar magnitudes of axial forces. However, in contrast to the transient transition change of axial forces observed at the stacked-layer interface during CFRP → Ti cutting, the transition time in the Ti → CFRP cutting direction was relatively longer. Considering that it is caused by the exit burr of the titanium alloy layer at the interface. In addition, the axial high-frequency contact

separation generated under ultrasound-assisted conditions resulted in a more stabilized axial force throughout the hole-making process of the stacked material, which was particularly evident in the cutting stage of the CFRP layer.

Figure 9 illustrates the influence of tangential feed per tooth and spindle speed on the axial force during ultrasonically assisted spiral milling of CFRP/Ti laminated material, considering different cutting sequences. Comparing the two cutting sequences, cutting from the Ti6Al4V layer results in slightly lower axial force than cutting from the CFRP layer. This can be attributed to the removal process of Ti6Al4V chips. When cutting from the Ti6Al4V layer, eccentric machining creates sufficient space for quick upward discharge of titanium alloy chips from the hole groove. On the

other hand, cutting from the CFRP layer causes Ti6Al4V chips to compress and rub against the hole wall of CFRP, leading to an increase in cutting force. In addition, the overall trend of axial forces in CFRP and titanium alloys is progressively more significant as the tangential feed per tooth f_z increases. When $f_z > 0.05$ mm/z, The reduction in the axial force of the titanium layer can be attributed to the increase in feed reducing the adhesion of the titanium alloy to the tool, as shown in Fig. 10. As the rotational speed n rises, there is a noticeable trend of decreasing axial force observed for the CFRP and titanium alloy; when $n = 5000$ r/min, the axial force of titanium alloy layer has a sudden increase, and the reason is analysed because this speed range is the speed range in which the chip tumour on the cutting edge is easy

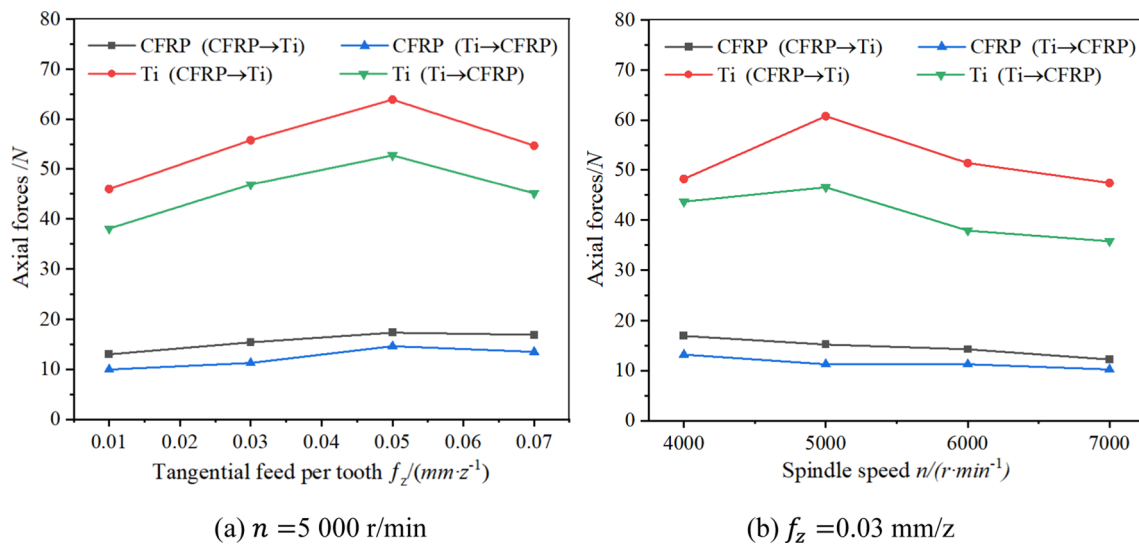


Fig. 9 Effect of tangential feed per tooth and spindle speed on the axial force in the hole making for different cutting sequences: **a** Spindle speed $n = 5000$ r/min, **b** Tangential feed per tooth $f_z = 0.03$

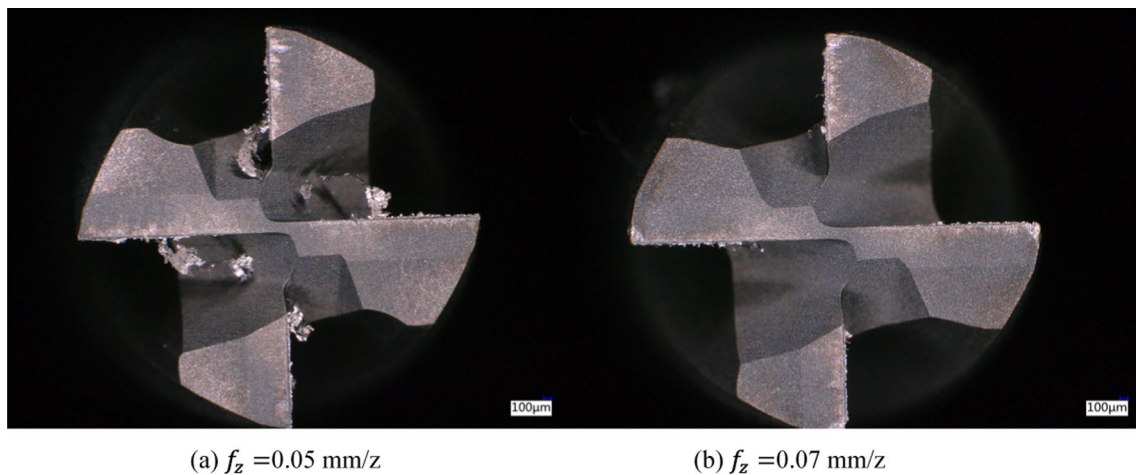


Fig. 10 Adhesion of titanium alloy to the tool at different feeds per tooth

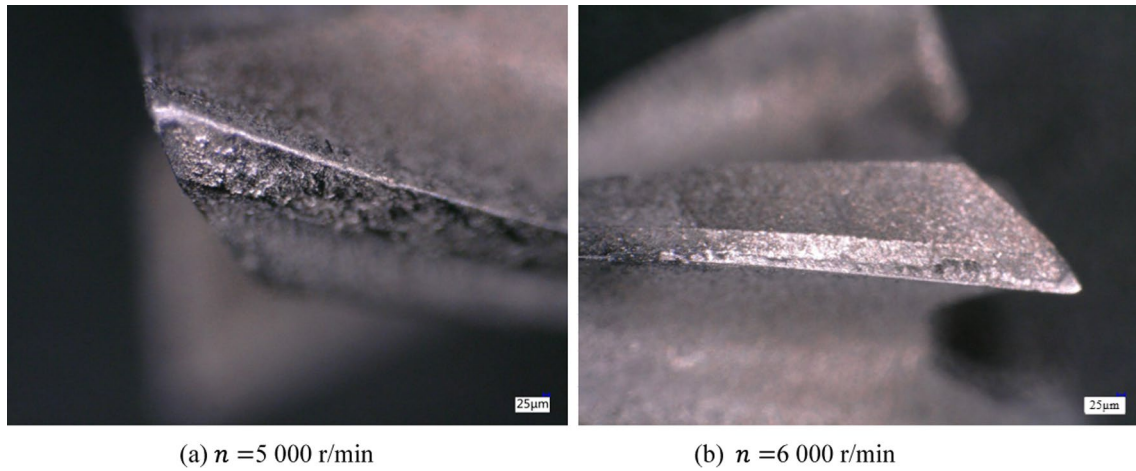


Fig. 11 Size of Chip Tumour on Cutting Edge at Different Spindle Speeds

to accumulate. The reason for this is that this speed range is the speed range in which the chip tumour on the cutting edge tends to accumulate. As the spindle speed is further increased, the cutting speed is increased, the workpiece and the wear coefficient of the front face is reduced, and the degree of chip deformation is reduced, and the chip tumour is dislodged, so the cutting force is reduced, as shown in Fig. 11.

4.2 Chip Pattern

One of the essential purposes of introducing the ultrasonic-assisted spiral hole milling process is to control the chip shape and to realize the effect of promoting chip breaking

and chip removal with the intermittent cutting process of the circumferential edge of the spiral hole milling and the eccentric machining method. In order to investigate the real impact of the cutting sequence on chip breaking and chip removal effectiveness in titanium alloy machining, we collected several titanium alloy chips from ordinary spiral milling holes and ultrasonically-assisted spiral milling holes under different cutting sequences in the test. We compared the chip morphology, as shown in Fig. 12.

By conducting a comparative analysis, it becomes evident that cutting from the CFRP side results in dark-colored, rough-textured chips. This is caused by the interaction between the Ti6Al-4V chips and the CFRP hole wall during the discharging process, leading to severe crushing and

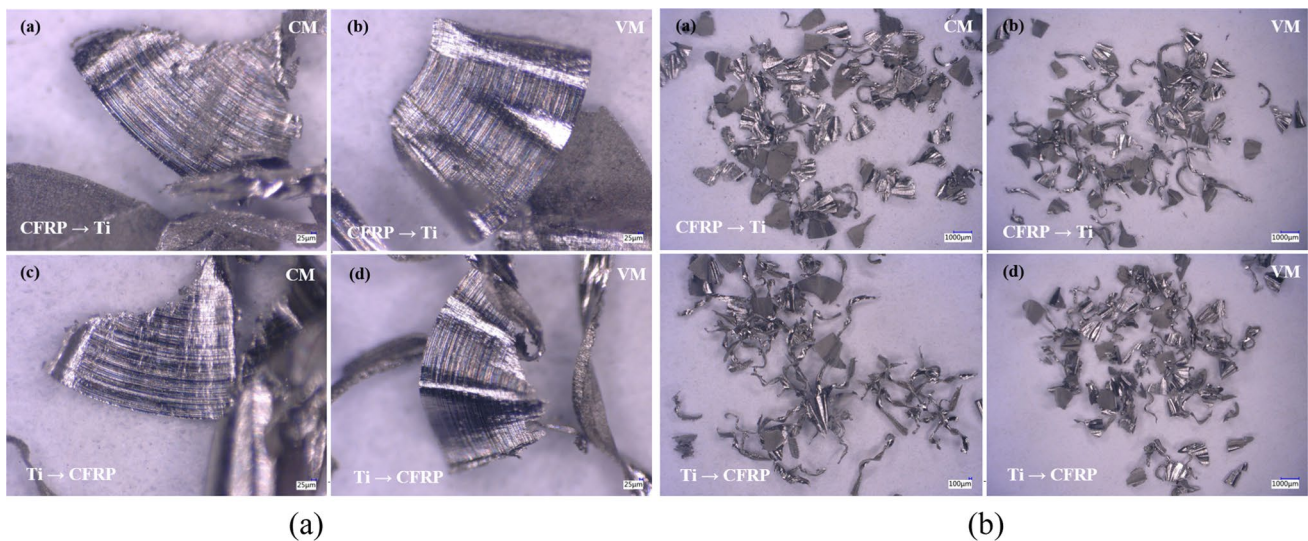


Fig. 12 Microscopic morphology of chips under different cutting sequences: **a** Two-dimensional chip morphology, **b** Three-dimensional chip pattern

deformation behaviour. Consequently, some carbon fibers and resin residues adhere to and remain on the Ti6Al4V chips. In contrast, cutting from one side of the Ti6Al4V produces a neat, regular Ti6Al4V chip shape with a clean and tidy surface and no carbon fibre or resin residues. This indicates that the hole surface of the CFRP layer is free of compression and scratches, allowing for a more efficient chip removal process. In addition, observing the above titanium alloy chip topography, it can be found that the titanium alloy chips under normal spiral milling are C-shape crushed chips, which are small in size and easy to be discharged quickly with the chip removal groove. Titanium alloy chips under ultrasonic-assisted helical milling are similar to those under ordinary helical milling, and are also C-shaped chips, with a finer length than that of ordinary helical milling, which is due to the high-frequency vibration caused by the axial vibration of ultrasonic-assisted helical milling, resulting in a certain degree of geometrical chip breakage. In addition, as can be seen from the ultrasonic depth-of-field observation of titanium chips, the surface of titanium chips under normal spiral milling conditions showed a single-direction texture. In contrast, the titanium alloy chips under ultrasound-assisted conditions showed a grid-like texture in two directions, and the chip surface was accompanied by obvious traces of ploughing, which increased the possibility of chip breakage to a certain extent. The above comparison of chip morphology shows the actual effect of ultrasonic-assisted machining on the cutting process more intuitively.

4.3 Hole-Making Quality

4.3.1 Interface Zone Damage

During hole-making in CFRP/Ti stacks, the CFRP-Ti interface is susceptible to different types of damage, with the specific mechanisms varying based on the cutting sequence. When initiating the cut from the CFRP layer, the primary cause of interface damage is the presence of residual Ti6Al4V chips remaining in the hole. The situation worsens due to the gap between the CFRP and Ti6Al4V layers, which hinders effective chip removal and leads to more severe erosion damage. Moreover, the interface region of the CFRP experiences thermal damage due to the high temperature of the Ti6Al4V chips during milling. This arises because the Ti6Al4V chips carry away most of the cutting heat and directly contact the CFRP hole surface. Conversely, cutting from the Ti6Al4V layer allows for smoother chip removal without impacting the CFRP layer [18]. However, the high cutting temperature of the titanium layer causes thermal damage to the resin fibers on the surface layer of the CFRP, making the cutting heat generated during this process the primary reason for damage to the CFRP interface and hole.

To sum up, the cutting sequence significantly affects the nature and extent of damage experienced by the CFRP/Ti interface during hole-making. The presence of residual chips, gap hindrance, and the contact between hot chips and the CFRP surface play crucial roles when cutting from the CFRP layer. At the same time, excessive cutting temperature becomes the critical factor in damaging the CFRP interface and hole during cutting from the Ti6Al4V layer.

The impact of the cutting sequence on hole-making quality in the interface zone is evident when reviewing Tables 3 and 4. During the cutting process with the sequence of Ti → CFRP, the interfacial ablative thermal damage occurred under both parameter conditions, both in the regular spiral milling and ultrasonic-assisted spiral milling methods. Under the cutting conditions of spindle speed $n = 7000$ rpm and tangential feed per tooth $f_z = 0.05$ mm/z, visible yellow damage is evident around the circumference of the hole edge in the interface zone. This occurrence is typically a consequence of ablative oxidation of the resin under high-temperature conditions, leading to discoloration. As a result, the oxidized and discolored resin experiences degradation, significantly diminishing the adhesive strength between the resin and carbon fibers. This phenomenon was also mentioned in [40], where different levels of damage rings were observed at the bonding surface when drilling CFRP/titanium alloy laminated structures with different material tools. In the ultrasonic-assisted spiral milling process, compared with the traditional drilling of holes, the cutting force is greatly reduced, and the chips are smaller and easy to be discharged, the heat dissipation is faster, and the cutting heat is greatly reduced, and the damage ring or even burn defects only appear when the cutting parameters are not suitable or the chip removal is not smooth. So when processing the stacked structure, especially when the large thickness of the material, chip removal is a problem that can not be ignored.

The CFRP → Ti cutting sequence resulted in reduced interfacial damage to the CFRP compared to CFRP → Ti cutting sequence resulted in reduced interfacial damage to the CFRP compared to the Ti → CFRP cutting sequence. This is due to the fact that the Ti at the bottom serves as a support pad for the CFRP, which reduces the entrance and exit damage of the CFRP to a certain extent. Moreover, when comparing holes created using the same cutting sequence and parameters, it was observed that ultrasonically-assisted spiral milling resulted in slightly better hole edge quality at the interface compared to regular spiral milling. Nan et al. in [17] pointed out that for CFRP/Ti alloy laminated holes, high temperature and high hardness titanium alloy swarf can cause serious erosion of CFRP under high feed conditions. This suggests that the ultrasonically-assisted condition has a certain inhibiting effect on temperature damage and chip damage phenomena at the hole exit.

Table 3 Effect of tangential feed per tooth on interface morphology for different cutting sequences

Cutting sequence	Tangential feed per tooth f_z (mm/z)			
	0.01	0.03	0.05	0.07
CFRP→Ti (CM)				
CFRP→Ti (VM)				
Ti→CFRP (CM)				
Ti→CFRP (VM)				

Table 4 Effect of spindle speed on interface morphology for different cutting sequences

Cutting sequence	Spindle speed n (Rom)			
	4000	5000	6000	7000
CFRP→Ti (CM)				
CFRP→Ti (VM)				
Ti→CFRP (CM)				
Ti→CFRP (VM)				

4.3.2 Bore Diameter and Roundness

CFRP thermal expansion coefficient and elastic recovery are significant, and shrinkage often exists in the process of CFRP hole-making. Titanium alloy has slight elastic

recovery, rebound during processing, and dimensional instability. During the process of integrated hole-making in CFRP/Ti–6Al–4 V laminated structures, variations in the elastic recovery of the two materials result in inconsistent hole diameter errors. This inconsistency can significantly

impact the assembly accuracy and lifespan of the laminated structure. Hence, it is crucial to closely examine CFRP and titanium alloy's hole diameter and roundness errors as critical parameters. Considering the effect of machining residual stresses, for this reason, the hole diameter and roundness of the machined workpieces were measured after one week of standing in a room temperature environment.

Figure 13 illustrates the relationship between hole diameter, roundness, tangential feed per tooth, and spindle speed for the CFRP → Ti cutting sequence. The impact of cutting parameters on hole-making accuracy is evident, particularly at the CFRP entrance, where a larger diameter and roundness are observed. This is mainly due to the pronounced scratching effect of Ti6Al4V chips on the CFRP hole surface during high cutting rotation. In contrast, the cutting parameters remained almost constant for the diameter and roundness of the Ti6Al4V layer. Furthermore, the difference in entrance

diameter between the CFRP layer and the Ti6Al4V layer becomes more significant with increasing feed rate. This phenomenon is associated with the thicker Ti6Al4V chips formed at higher feed rates, intensifying their potential to damage the CFRP orifice surface. To minimize damage to the CFRP orifice surface, we recommended a lower feed rate in industrial production. While hole roundness is relatively less affected by cutting parameters compared to hole diameter, an increase in feed and cutting speed tends to elevate the roundness of the hole. Kuo et al. in [41] also illustrated that the surface roughness of holes of different materials increases with the increase in cutting speed. Therefore, the feed and cutting speed should be reduced during the finishing stage of the holes to minimise the damage to the CFRP layer by the Ti6Al4V chips and to improve the hole accuracy.

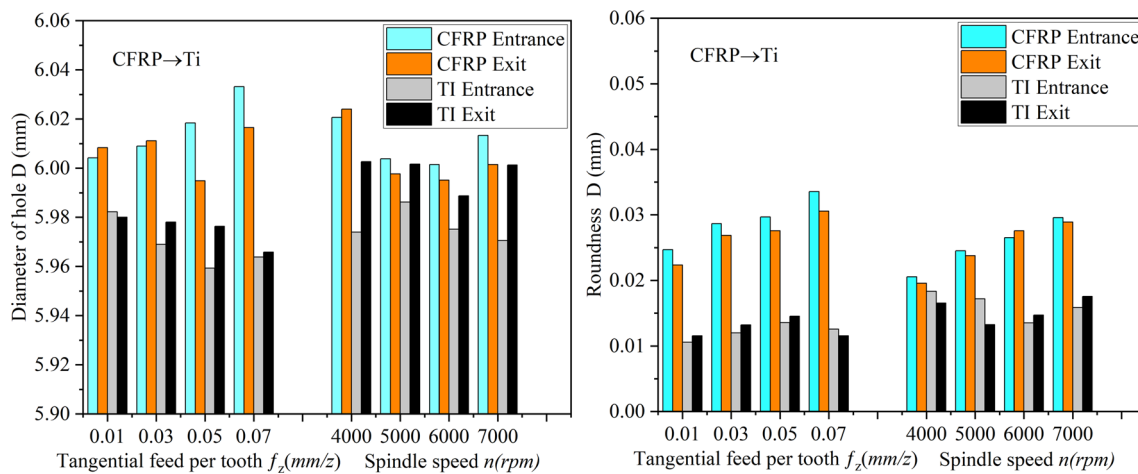


Fig. 13 Variation of hole diameter and roundness with cutting parameters for CFRP → Ti cutting sequence

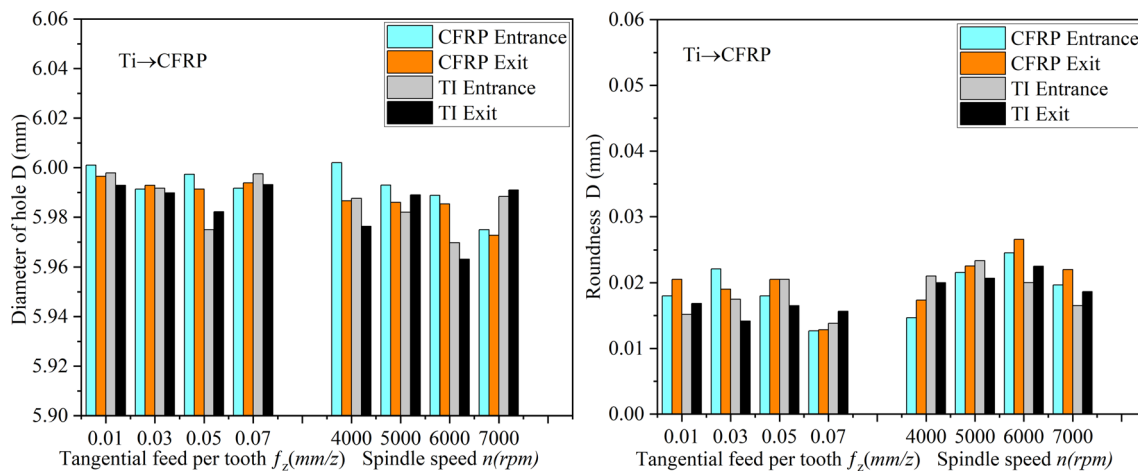


Fig. 14 Variation of hole diameter and roundness with cutting parameters for Ti → CFRP cutting sequence

Figure 14 depicts the relationship between tangential feed per tooth, spindle speed, hole diameter, and roundness for the Ti → CFRP cutting sequence. The machining parameters have minimal impact on hole accuracy. The inlet and outlet diameters of the CFRP layer remain relatively constant, which confirms the erosion damage caused by Ti6Al4V chips during the cutting process from the CFRP → Ti side. Hence, for dimensional and geometrical accuracy considerations, we can choose the Ti → CFRP cutting sequence.

4.3.3 CFRP Hole Entrance and Exit Quality

In the hole-making process of CFRP/Ti stacks, the internal machining factors of CFRP affect its hole-making quality. In addition, it is related to the hole-making temperature of the titanium alloy and the shape of the titanium alloy chip. This subsection focuses on analyzing the quality of the CFRP hole inlet and outlet.

Figure 15 illustrates how the tearing factor changes concerning tangential feed per tooth and spindle speed in the CFRP → Ti cutting sequence. The CFRP hole exhibits a higher entrance tearing than the exit tearing factor. This disparity arises from the beneficial support the underlying titanium alloy layer provides during the hole-making process, effectively reducing the likelihood of tearing at the hole's exit. The overall hole exit and entrance tear factors for both machining methods increased with the increase of tangential feed per tooth and decreased with the growth of spindle speed [27]. In addition, the entrance/exit tearing factor for the ultrasonically assisted spiral milling condition is overall more minor than that of the regular spiral milling. This is because the ultrasonic assisted effectively removes the CFRP and also changes the shape of the titanium alloy chips, and

reduces the chip size to a certain extent, which promotes the chip breakage and chip removal to a certain extent, and thus reduces the damage of the titanium alloy chips to the CFRP hole wall, and then effectively inhibits the tearing damage of the CFRP entrance. This further illustrates the problem of titanium chips damaging the pore wall quality of the CFRP layer and triggering delamination as proposed by BRINKS-MEIER et al. in [42] as they are discharged out of the pore.

In Fig. 16, the tearing factor is plotted against the feed per tooth in the tangential direction and the spindle speed for the Ti → CFRP cutting sequence. Observing the Ti → CFRP cutting hole sequence, it becomes evident that the risk of exit tearing damage in the CFRP layer is somewhat elevated. This is attributed to the loss of support from the lower titanium alloy mat during the process, and the degree of exit tearing is greater than that of entrance tearing under this cutting direction.

In the experimental range of both cutting parameters, the ultrasound-assisted condition plays a good role in improving the CFRP entrance and exit quality. By comparing the tearing factor of the two cutting directions, the quality of the titanium side cut under ultrasonically assisted conditions can reach the quality of the CFRP side cut of regular spiral milling. The comparison indicates that the ultrasound-assisted spiral milling method can achieve improved entrance and exit quality when following the cutting sequence of Ti → CFRP. This addresses, to some extent, the issue of significant tearing at the exit of the titanium alloy side entry in CFRP/Ti stacked materials. However, in terms of the tearing damage itself, the CFRP → Ti cutting sequence with ultrasonic-assisted spiral milling can achieve higher entrance/exit quality.

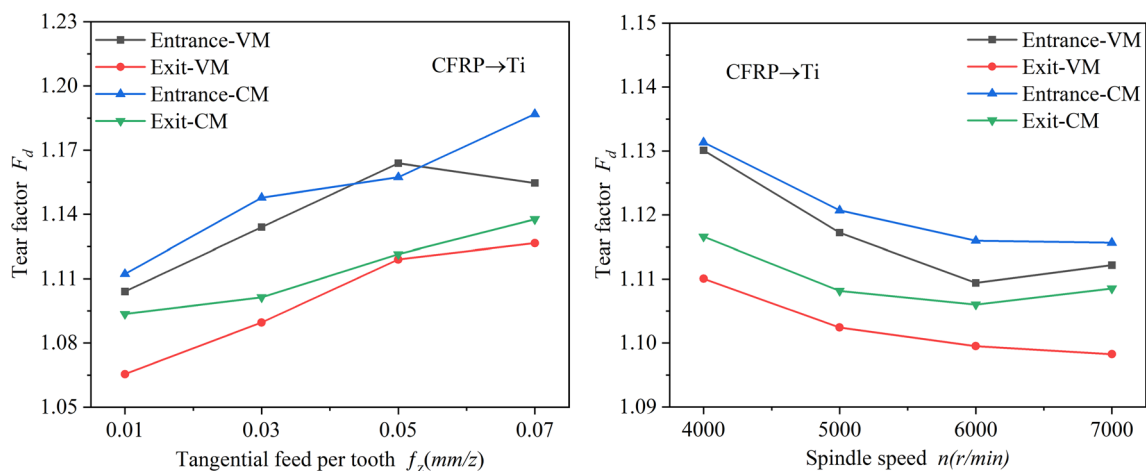


Fig. 15 Variation of tearing factor with tangential feed per tooth and spindle speed for CFRP → Ti cutting sequence

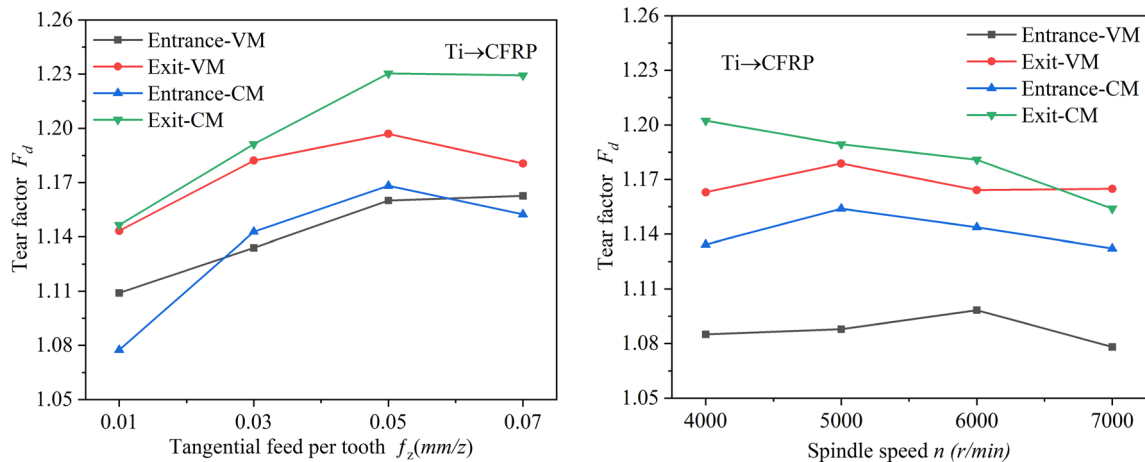


Fig. 16 Variation of tearing factor with tangential feed per tooth and spindle speed for Ti → CFRP cutting sequence

5 Conclusions

This paper presents a comprehensive experimental study on CFRP/titanium overlays' milling process to thoroughly investigate how the milling hole-making sequence influences the cutting response. The primary machining responses related to the cutting conditions, including milling forces, chip morphology, and hole-making quality (e.g., damage in the interface region, hole accuracy, and roundness), were meticulously documented. The key findings drawn from the results are as follows.

- The cutting sequence selection dramatically influences the magnitude of the axial force. When cutting the CFRP/Ti stacks from the CFRP layer, the maximum axial force value is higher than cutting from the Ti6Al4V layer. Compared to regular spiral milling, the average axial force was significantly lower in the ultrasound-assisted spiral milling condition, and the transition of axial force at the interface of the stacked layer was more stable. Still, the overall range of fluctuation of axial force increased.
- The high-frequency vibration in the axial direction under ultrasound-assisted conditions caused the chips to show a grid-like texture in both directions, with evident plowing traces, effectively promoting the chip breaking of titanium alloy.
- The cutting sequence strongly influences the quality of hole-making. From the titanium alloy side cut into the hole size accuracy and consistency is good, ultrasound-assisted conditions of the titanium alloy side cut into the entrance and exit quality can basically reach the level of quality of the ordinary spiral milling CFRP side cut, ultrasound-assisted conditions for the quality of the hole-making played a good role in improving the quality of the hole.

- The tearing factor at the entrance and exit of the hole cut from the titanium layer was overall greater than that in the CFRP direction. In addition, the tearing factor at the entrance and exit of the CFRP hole increases with the increase of feed per tooth in the tangential direction and decreases with the increase of spindle speed for both machining methods.

In this paper, preliminary conclusions on the feasibility of CFRP/Ti–6Al–4 V stacked materials in the Ti → CFRP cutting direction under ultrasound-assisted helical milling conditions have been drawn through experimental studies, but there is still a certain risk of exit tear damage in this cutting direction, and the process parameters of ultrasound-assisted helical milling can be targeted and explored in order to reduce the risk of exit damage.

Future research can also be combined with the following aspects:

1. In the stacked hole making cutting environment. Green manufacturing is the development trend of today's manufacturing industry [43, 44]. In addition to the tool, cutting parameters, processing methods and other factors, the cutting environment and other external factors are also affecting the quality of the hole-making key. MQL compared with dry cutting can significantly reduce tool wear, improve tool life and its processing quality, and is gradually being widely used in the CFRP/Ti stacked material holemaking, but there is still the problem of poor cooling capacity. Nanofluidic micro lubrication (NMQL) is a new cooling method, which solves the technical bottleneck of insufficient cooling capacity of MQL [45]. The application of NMQL cooling method to the problem of CFRP/Ti stacked material hole making aims to optimise the cutting environment of stacked hole

making, increase tool life, improve the quality of hole making, which is of great significance to the green hole making processing of CFRP/Ti stacked material.

- In improving the assembly quality of laminated holes. Relevant research shows that a certain regular surface morphology of the hole wall can improve the assembly quality of the hole wall and fasteners, so that the contact surface of the two forces are more uniform, and the fatigue life is higher. For CFRP/titanium alloy laminated materials, fatigue failure in the connection part is the main cause of accidents, so it is of great significance and practical value to carry out research on the surface morphology of the hole wall of laminated materials in order to improve the performance of the connection part and its fatigue life, and to enhance the safety of the laminated components.

Acknowledgements The authors acknowledge the technical staff of our research laboratory for their assistance in carrying out the experiments.

Author Contributions Conceptualization, JP and KY; methodology, JP and KY; software, JP; validation, JP and ZC; formal analysis, JP; investigation, YZ; resources, ZC; data curation, YZ; writing—original draft preparation, KY; writing—review and editing, KY and ZC; visualization, JP; supervision, ZC and JP; project administration, ZC; funding acquisition, ZC. All authors have read and agreed to the published version of the manuscript.

Funding This research received no external funding.

Data Availability The data presented in this study are available in the article.

Declarations

Conflict of interest The authors declare that they have no known competing financial interests or personal relationships that could have appeared to influence the work reported in this paper.

Ethics Approval and Consent to Participate Not applicable.

Informed Consent Not applicable.

References

- Liu, C., Ren, J., Zhang, Y., et al. (2023). The effect of tool structure and milling parameters on the milling quality of CFRP based on 3D surface roughness. *International Journal Precision Engineering Manufacturing-Green Technology*, 24, 931–944.
- Xu, J. Y., Lin, T. Y., Li, L. F., Ji, M., Davim, J. P., Geier, N., & Chen, M. (2022). Numerical study of interface damage formation mechanisms in machining CFRP/Ti6Al4V stacks under different cutting sequence strategies. *Composite Structures*, 285, 115236.
- Zhao, M., Wang, F. J., Fu, R., Sun, K., Du, C. L., & Cui, J. C. (2023). Drilling study on CFRP/Al stack with different CFRP thickness using chip-breaking step drill bit. *Journal of Manufacturing Processes*, 90, 300–309.
- Grilo, T. J., Paulo, R. M. F., Silva, C. R. M., & Davim, J. P. (2013). Experimental delamination analyses of CFRPs using different drill geometries. *Composites Part B: Engineering*, 45(1), 1344–1350.
- Wang, F. J., Qian, B. W., Jia, Z. Y., Fu, R., & Cheng, D. (2017). Secondary cutting edge wear of one-shot drill bit in drilling CFRP and its impact on hole quality. *Composite Structures*, 178, 341–352.
- Geier, N., Xu, J. Y., Pereszlai, C., Poór, D. I., & Davim, J. P. (2021). Drilling of carbon fibre reinforced polymer (CFRP) composites: Difficulties, challenges and expectations. *Procedia Manufacturing*, 54, 284–289.
- Poór, D. I., Geier, N., Pereszlai, C., & Xu, J. Y. (2021). A critical review of the drilling of CFRP composites: Burr formation, characterisation and challenges. *Composites Part B: Engineering*, 223, 109155.
- Geier, N., Davim, J. P., & Szalay, T. (2019). Advanced cutting tools and technologies for drilling carbon fibre reinforced polymer (CFRP) composites: A review. *Composites Part A: Applied Science and Manufacturing*, 125, 105552.
- Pimenov, D. Y., Mia, M., & Gupta, M. K. (2021). Improvement of machinability of Ti and its alloys using cooling-lubrication techniques: A review and future prospect. *Journal of Materials Research and Technology*, 11, 719–753.
- Jiao, A., Yuan, J., Zhang, Y., et al. (2023). Study on variable parameter helical milling of TC4 titanium alloy tube. *International Journal of Precision Engineering and Manufacturing*, 24, 1947–1959.
- Xu, J., Mansori, M. E., & Voisin, J. (2019). On the interpretation of drilling CFRP/Ti6Al4V stacks using the orthogonal cutting method: Chip removal mode and subsurface damage formation. *Journal of Manufacturing Processes*, 44, 435–447.
- Yu, B., He, P., & Jiang, Z. (2017). Interlaminar fracture properties of surface treated Ti-CFRP hybrid composites under long-term hygrothermal conditions. *Composites Part A: Applied Science and Manufacturing*, 96, 9–17.
- Wang, C.-Y., Chen, Y.-H., An, Q.-L., Cai, X.-J., Ming, W.-W., & Chen, M. (2015). Drilling temperature and hole quality in drilling of CFRP/aluminum stacks using diamond coated drill. *International Journal of Precision Engineering and Manufacturing*, 16(8), 1689–1697.
- Kim, D., Beal, A., & Kwon, P. (2016). Effect of tool wear on hole quality in drilling of carbon fiber reinforced plastic-titanium alloy stacks using tungsten carbide and polycrystalline diamond tools. *Journal of Manufacturing Science and Engineering-Transactions of the ASME*, 138(3), 031006.
- Wei, J. C., Jiao, G. Q., Jia, P., & Huang, T. (2013). The effect of interference fit size on the fatigue life of bolted joints in composite laminates. *Composites Part B: Engineering*, 53, 62–68.
- Alagan, N. T., Sajja, N. T., Gustafsson, A., Savio, E., Ghiotti, A., Bruschi, S., & Bertolini, R. (2023). Investigation of the quality of Al-CFRP stacks when drilled using innovative approaches. *CIRP Journal of Manufacturing Science and Technology*, 43, 260–272.
- Nan, C. G., Wu, D., & Ma, X. G. (2016). Study on the drilling quality of carbon fiber reinforced plastic and titanium stacks. *Journal of Mechanical Engineering*, 52(11), 177–185. in Chinese.
- An, Q. L., Dang, J. Q., Li, J. L., Wang, C. Y., & Chen, M. (2020). Investigation on the cutting responses of CFRP/Ti stacks: With special emphasis on the effects of drilling sequences. *Composite Structures*, 253, 112794.
- Dahnel, A. N., Ascroft, H., & Barnes, S. (2020). An investigation of hole quality during drilling of carbon fibre reinforced plastic and titanium (Ti6Al4V) using tungsten carbide drills. *Materials Today: Proceedings*, Part, 1(29), 161–167.
- Xu, J. Y., Li, C., Chen, M., Mansori, M. E., & Davim, J. P. (2020). On the analysis of temperatures, surface morphologies and tool

- wear in drilling CFRP/Ti6Al4V stacks under different cutting sequence strategies. *Composite Structures*, 234, 111708.
21. Xu, Y. M., Li, H. G., Yang, Y. F., Hu, Y. B., & Tao, J. (2019). Determination of residual stresses in Ti/CFRP laminates after preparation using multiple methods. *Composite Structures*, 210, 715–723.
 22. Luo, B., Zhang, K., Liu, S., Cheng, H., & Wang, R. X. (2019). Investigation on the interface damage in drilling low-stiffness CFRP/Ti stacks. *Chinese Journal of Aeronautics*, 32(9), 2211–2221.
 23. Xu, J. Y., & Mansori, M. E. (2016). Numerical modeling of stacked composite CFRP/Ti machining under different cutting sequence strategies. *International Journal of Precision Engineering and Manufacturing*, 17(1), 99–107.
 24. Xu, J. Y., Mkaddem, A., & El Mansori, M. (2016). Recent advances in drilling hybrid FRP/Ti composite: A state-of-the-art review. *Composite Structures*, 135, 316–338.
 25. Hocheng, H., & Puw, H. Y. (1992). On drilling characteristics of fiber-reinforced thermoset and thermoplastics. *International Journal of Machine Tools and Manufacture*, 32(4), 583–592.
 26. Kim, D., Ramulu, M., & Doan, X. (2005). Influence of consolidation process on the drilling performance and machinability of PIXA-M and PEEK thermoplastic composites. *Journal of Thermoplastic Composite Materials*, 18(3), 195–217.
 27. Wang, B., Wang, Y. F., Zhao, H., Sun, L., Wang, M. H., & Kong, X. J. (2020). Effect of a Ti alloy layer on CFRP hole quality during spiral milling of CFRP/Ti laminate. *Composite Structures*, 252, 112670.
 28. Dong, H. Y., Chen, G. L., Zhou, L., et al. (2017). Processing research on orbital drilling of CFRP/Ti–6Al–4V stacks. *Acta Materiae Compositae Sinica*, 34(03), 540–549. in Chinese.
 29. Wang, H. Y., Qin, X. D., Li, H., & Ren, C. Z. (2013). Analysis of cutting forces in spiral milling of carbon fiber-reinforced plastics. *Proceedings of the Institution of Mechanical Engineers, Part B: Journal of Engineering Manufacture*, 227(1), 62–74.
 30. Denkena, B., Boehnke, D., & Dege, J. H. (2008). Spiral milling of CFRP–titanium layer compounds. *CIRP Journal of Manufacturing Science and Technology*, 1(2), 64–69.
 31. Sun, J., Li, P. Y., Zhang, S., Chen, Y. S., Lu, H., Chen, G. Q., & Shao, D. (2023). Simulation and experimental study of ultrasonic vibration-assisted milling of GH4169 high-temperature alloy. *Alexandria Engineering Journal*, 73, 403–413.
 32. Joshi, R. S., & Singh, H. (2014). An investigation on flank wear mechanism of tungsten carbide drills during conventional and modulation assisted drilling. *Machining Science and Technology*, 18(1), 99–119.
 33. Li, Y. Z., Zhang, D. Z., Wang, H., Ye, G. H., He, R., & Cong, W. L. (2022). Theoretical and experimental investigations on rotary ultrasonic surface micro-machining of brittle materials. *Ultrasonics Sonochemistry*, 89, 106162.
 34. Cong, W. L., Pei, Z. J., Deines, T. W., Liu, D. F., & Treadwell, C. (2013). Rotary ultrasonic machining of CFRP/Ti stacks using variable feedrate. *Composites Part B: Engineering*, 52, 303–310.
 35. Cong, W. L., Pei, Z. J., & Treadwell, C. (2014). Preliminary study on rotary ultrasonic machining of CFRP/Ti stacks. *Ultrasonics*, 54(6), 1594–1602.
 36. Yan, C. R., Chen, Y., Qian, N., et al. (2022). Adaptive approaches to identify the interface in low frequency vibration-assisted drilling of CFRP/Ti6Al4V stacks. *International Journal of Precision Engineering and Manufacturing*, 23(8), 895–909.
 37. Onawumi, P. Y., Roy, A., Silberschmidt, V. V., & Merson, E. (2018). Ultrasonically assisted drilling of aerospace CFRP/Ti stacks. *Procedia CIRP*, 77, 383–386.
 38. Pecat, O., & Brinksmeier, E. (2014). Low damage drilling of CFRP/titanium compound materials for fastening. *Procedia CIRP*, 13, 1–7.
 39. Qin, S. Q., Zhu, L. D., Wiercigroch, M., Ren, T. Y., Hao, Y. P., Ning, J. S., & Zhao, J. Z. (2022). Material removal and surface generation in longitudinal-torsional ultrasonic assisted milling. *International Journal of Mechanical Sciences*, 227, 107375.
 40. Ramulu, M., et al. (2001). A study on the drilling of composite and titanium stacks. *Composite Structure*, 54(1), 67–77.
 41. Kuo, C. L., Soo, S. L., Aspinwall, D. K., Thomas, W., Bradley, S., Pearson, D., M'Saoubi, R., & Leahy, W. (2014). The effect of cutting speed and feed rate on hole surface integrity in single-shot drilling of metallic-composite stacks. *Procedia CIRP*, 13, 405–410.
 42. Brinksmeier, E., & Janssen, R. (2002). Drilling of multi-layer composite materials consisting of carbon fiber reinforced plastics (CFRP), titanium and aluminum alloys. *CIRP Annals-Manufacturing Technology*, 51(1), 87–90.
 43. Zou, F., Zhong, B. F., Zhang, H., An, Q. L., et al. (2022). Machinability and surface quality during milling CFRP laminates under dry and supercritical CO₂-based cryogenic conditions. *International Journal Precision Engineering Manufacturing-Green Technology*, 9(3), 765–781.
 44. Pal, A., Chatha, S. S., & Sidhu, H. S. (2022). Performance evaluation of various vegetable oils and distilled water as base fluids using eco-friendly MQL technique in drilling of AISI 321 stainless steel. *International Journal Precision Engineering Manufacturing-Green Technology*, 9(3), 745–764.
 45. Celis, P., Vazquez, E., Soria-Hernández, C. G., et al. (2022). Evaluation of ball end micromilling for Ti6Al4V ELI microneedles using a nanoadditive under MQL condition. *International Journal Precision Engineering Manufacturing-Green Technology*, 9(5), 1231–1246.

Publisher's Note Springer Nature remains neutral with regard to jurisdictional claims in published maps and institutional affiliations.

Springer Nature or its licensor (e.g. a society or other partner) holds exclusive rights to this article under a publishing agreement with the author(s) or other rightsholder(s); author self-archiving of the accepted manuscript version of this article is solely governed by the terms of such publishing agreement and applicable law.



Kai Yang is a master's student at Suzhou University of Science and Technology. His research interest is the optimisation of machining process of composite materials.



Jie Pan is an assistant lecturer at Jiangsu United College of Vocational Technology, graduated from Suzhou University of Science and Technology with a Master of Engineering degree in Mechanical Manufacturing and Automation. His research interests include spiral milling process of composite materials and titanium alloys.



Ziyang Cao Yiwen Zhu is a master's student at Suzhou University of Science and Technology. His research interests are surface quality optimisation of titanium alloy micro-milling.



Ziyang Cao is a professor and deputy dean of the School of Mechanical Engineering, Suzhou University of Science and Technology. He graduated from Nanjing University of Aeronautics and Astronautics, majoring in mechanical manufacturing and automation, and received his Ph.D. degree, with his main research interests in high-efficiency precision machining technology and equipment.